Bioprinting 11 (2018) e00029

Contents lists available at ScienceDirect

Bioprinting

journal homepage: www.elsevier.com/locate/bprint

3D bioprinting of hydrogels for retina cell culturing

Pengrui Wang[a], Xin Li[b], Wei Zhu[c], Zheng Zhong[b], Amy Moran[c], Wenqiu Wang[b], Kang Zhang[b,*], Shaochen Chen[a,c,**]

[a] Materials Science and Engineering Program, University of California San Diego, La Jolla, CA 92093, USA
[b] Shiley Eye Institute and Department of Ophthalmology, University of California San Diego, La Jolla, CA 92093, USA
[c] Department of NanoEngineering, University of California San Diego, La Jolla, CA 92093, USA

ARTICLE INFO

Keywords:
3D bioprinting
Retina
Hyaluronic acid
Photoreceptors
Retinal-pigment epithelium
Compressive modulus

ABSTRACT

Recapitulating native retina environment is crucial in isolation and culturing of retina photoreceptors (PRs). To date, maturation of PRs remains incomprehensible *in vitro*. Here we present a strategy of integrating the physical and chemical signals through 3D-bioprinting of hyaluronic acid (HA) hydrogels and co-differentiation of retinal progenitor cells (RPCs) into PRs with the support of retinal-pigment epithelium (RPEs). To mimic the native environment during retinal development, we chemically altered the functionalization of HA hydrogels to match the compressive modulus of HA hydrogels with native retina. RPEs were incorporated in the culturing system to support the differentiation due to their regeneration capabilities. We found that HA with a specific functionalization can yield hydrogels with compressive modulus similar to native retina. This hydrogel is also suitable for 3D bioprinting of retina structure. The results from cell study indicated that derivation of PRs from RPCs was improved in the presence of RPEs.

1. Introduction

The retina is a complex light sensitive tissue that collects light before transmitting the information to brain for realizing the visual environment [1]. In human retinas, cells of specific functions are embedded in extra cellular matrix (ECM) following a multi-layered configuration [2]. These ECMs have specific chemical compositions and physical properties that could affect the functionality of cells residing in them. In human retina, the ECM consists mainly of hyaluronic acid (HA), which is a negatively charged polysaccharide [3]. Photoreceptor cells (PRs), which reside across the intermediate layers of retina, are responsible for light detection. Their degeneration could lead to the onset of blindness in numerous diseases, including retinitis pigmentosa and age-related macular degeneration (AMD) [4]. Regenerating healthy PRs in the eye is a promising strategy to treat these diseases. However, culturing of isolated PRs *in vitro* still remains challenging [5]. Unlike the whole retina, which can be maintained in culture for several days, the PRs undergo morphological changes and profound apoptosis in isolated culturing without the support of ECM and other cell types [6]. The few surviving cells lose their outer segments and downregulate the expression of visual cycle proteins [1]. Therefore, there is a growing need to develop a viable strategy to specifically culture PRs *in vitro* with ECM for biological studies such as drug screening, cell intervention and integration, and disease modeling. Furthermore, the discovery of a suitable ECM material for PRs culturing could help to study their maturation and realizing repair by implantation in the future.

Residing adjacent to the PRs in a similar ECM, retinal pigment epithelium (RPE) is a highly specialized cell with pigmented microvilli [7]. Research has shown the importance of RPE in nutrient transport, growth factor production, and phagocytosis of photoceptors [8]. Although quiescent under physiological condition in the eyes, the RPE cells will start to proliferate in response to traumatic injuries in retina [9]. Previous works have reported sequential development of both RPE and PRs from fetal retinal progenitor cells (fRPCs) [10]. This study has shown that the RPEs assembled a bilayer structure with the neural retina, which matured into PRs at an early stage of development. These findings inspired a strategy to regenerate damaged PRs with the support of RPEs. To realize this strategy, we aim to encapsulate cells with ECMs closely related to native retina and localize individual cell type following the same arrangement as the native retina. Our recent development in 3D bioprinting can construct different tissues through polymerization of cell-containing ECMs [11]. Unlike conventional planar maturation strategies, 3D bioprinting could create mechanical and geometrical cues that closely resemble the cell niche [1,12]. In previous works, we have demonstrated 3D

* Corresponding author.
** Corresponding author at: Department of NanoEngineering, University of California San Diego, La Jolla, CA 92093, USA.
E-mail addresses: chen168@eng.ucsd.edu (K. Zhang), k5zhang@ad.ucsd.edu (S. Chen).

https://doi.org/10.1016/j.bprint.2018.e00029
Received 8 June 2018; Received in revised form 31 July 2018; Accepted 4 September 2018

bioprinting of hepatic and vascular system to regenerate functional tissues from embryonic stem cells [11,13]. The rapid and cell compatible printing process enabled us to create complex 3D structures while maintaining the viability of cells.

Recently, different strategies have been used to develop PRs from human pluripotent stem cells [14]. For example, Lorber et al. demonstrated 3D printing of retinal and glial cells as a retina model while Hunt et al. investigated the effect of stiffness on retinal differentiation [15]. Their results indicated that the differentiation was mostly enhanced in ECMs that mimic the stiffness of the native retina. While these studies have shown the efforts of maturing PRs *in vitro*, recapitulating surrounding environments of the cells such as stiffness and cell hierarchy during differentiation still remain challenging [12]. Mitrousis et al. reported the use of HA in encapsulation of retinal stem cells (RSCs) to improve PR growth [1]. As an abundantly present polysaccharide in the subretinal space, HA is responsible for sequestration and presentation of biomolecules to PRs. It has been reported to facilitate PR maturation by upregulation of the mTOR pathway in RSCs [1]. While native HA does not form a physically stable gel with cells, several chemical modification methods have been reported to functionalize the HA with methacrylation by glycidyl-hydroxyl reaction, resulting in a photopolymerizable hydrogel (HA-GM) that can be 3D printed with our reported printing techniques [16].

In this work, we present a strategy to synthesize HA-GMs with different degrees of methacrylation (DM) by altering molar ratios of initial reagents. Their physical properties such as swelling ratio and compressive modulus are measured and analyzed. Furthermore, we have constructed a multi-layered tissue model using 3D bioprinting to resemble the native retina structure. The fetal retinal progenitor cells (fRPCs) were co-differentiated with RPEs to improve their differentiation.

2. Materials and methods

2.1. Materials Synthesis

HA-GMs were synthesized following protocols reported previously [11]. Briefly, 1 g of hyaluronic acid (Lifecore Biomedical, MN) was added into 100 ml of 50:50 acetone: water solution. The solution was mixed overnight before adding triethylamine and equal amount of glycidyl methacrylate with a designated molar ratio. The reaction was continued for 24 h before dialysis over distilled water for 24 h. The resulting solution was dried by lyophilization (Labconco) over 5 days before rehydrated to make a hydrogel solution. 10 mg of the dried hydrogel was dissolved in 1 ml of deuterium oxide completely and examined by ^{1}H NMR (ECA 500, JEOL USA).

To improve cell binding of HA-GM, we introduced long chain Arg-Gly-Asp-Ser (RGDS) peptide (American Peptides) into the hydrogel. The polypeptide was synthesized by EDC-NHS synthesis with polyethylene glycol following previously reported protocols [17]. PEG-RGDS was mixed with HA-GM hydrogel in 2 mM/ml concentration [18]. The photoinitiator, lithium phenyl-2,4,6 trimethylbenzoylphosphinite (LAP) was synthesized following previously published protocols [11]. Briefly, dimethyl phenylphosphonite was mixed with equal amount of 2,4,6-trimethylbenzoyl chloride overnight. The reaction was conducted over 18 h under inert gas before heated to 50 °C. Lithium bromide was mixed with 2-butanone and added into the solution slowly over ten minutes before cooled to room temperature over four hours. The precipitates were filtered and washed with 2-butanoe before dried by vacuum.

2.2. Physical and mechanical properties assessment

To analyze the microstructure of the HA-GMs by scanning electron microscopy (SEM), the printed HA-GM hydrogels were dried over a series of ethanol/water solutions with an increasing ethanol concentration. The hydrogels were further dried by hexamethyldisilazane. After completely removal of any solvents, the samples were sputtered with iridium for 7 s and then imaged with SEM (Zeiss Sigma 500). The SEM images were used to evaluate the average pore sizes and interconnections between pores.

To analyze the physical properties such as swelling ratio of the HA-GMs with different degrees of methacrylation (DMs), the hydrogels were printed into cylindrical shape with the same dimensions, exposure duration and light intensity. The samples were then incubated in saline solution at 37 °C for 1 day, 3 days and 7 days before being tested. Images were taken to evaluate the swelling ratio of the hydrogels. The porosities of the hydrogels were calculated by swelling factors and polymer volumes. The mechanical properties of HA-GM hydrogels were evaluated by compression test using MicroSquisher (CellScale) at 10% strain and 2 μm/s strain rates. The instrument collected the force and displacement data, which were further analyzed using an in-house software to calculate the compressive modulus. The diameter and height changes of each hydrogel were measured by a microscope over 7 days to analyze the volumetric swelling ratio of each sample.

2.3. RPEs encapsulation

RPEs were purchased from ATCC and cultured according to manufacturer's guide. The RPE cells were cultured to passage 7 before digested to mix with HA-GMs with 500k/ml concentration in the final cell-gel mixture. The mixture was printed and continuously cultured over the course of 10 days. Ethidium homodimer and calcein AM were used to analyze the viability of RPEs encapsulated in different HA-GMs. The viability of RPE cells were calculated as the ratio of number of live cells over total number of cells.

2.4. Multilayered printing

To build a layer-by-layer structure with hydrogel-cell matrix, we developed a rapid 3D printing process to consecutively construct each layer. Briefly, a light source of 365 nm wavelength (Omnicure S2000, Waltham, MA) was used to provide the UV light for photo-polymerization. Structures were designed by Solid Works ®, which were then converted to digital mask patterns and transferred to the digital-mirror array device (DMD) chip by in-house software. The DMD chip was used as an optical mask for projecting patterns onto the solution containing hydrogel, cell, and photoinitiator. Once the light passes through the lenses, it is collimated to form a precise image on the solution, where polymerization occurs to form the structure. The RPEs mixed with HMHA-GM for the first layer was loaded on the reservoir of the stage, which moves in all three directions guided by the computer. After printing of the first pattern, the solution was washed away while the printed structure remained. The RPCs with HMHA-GM for the second layer was then loaded on top of the first layer, followed by lowering the stage. After the second layer is printed, the multi-layer structure was rinsed and put in culture for further analysis.

2.5. Co-differentiation of fRPCs

Human fetal retinal progenitor cells (fRPCs) were harvested from 20 to 24 weeks old fetus and maintained with growth medium (Ultra CULTURE™ serum-free medium, 10 ng/ml EGF, 20 ng/ml bFGF, 2 mM L-Glutamine and 50 μg/ml gentamin). The fRPCs were differentiated into PR cells following methods reported in a previous publication [19]. Briefly, after reaching 50% confluency, fRPCs were switched into PR differentiation medium (DMEM/F12: Neurobasal medium 1:1, N2, B27, 0.05% BSA Fraction V; 2 mM Glutamax, 50 nM docosahexaenoic acid and supplemented with 1 μM IWP2, 10 μM DAPT, 100 nM purmorphamine, 100 nM retinoic acid, 100 μM Taurin, 10 ng/ml bFGF) for two weeks. The cells were mixed with

HMHA-GM at 500k/ml concentration in the final cell-gel mixture for printing.

3. Results and discussions

3.1. Methacrylation of HA-GM

The physical properties such as stiffness of the hydrogels is closely related to the degree of crosslinking, which is affected by the number of methacrylate groups attached to the polymer backbone. This number can be quantified as degree of methacrylation (DM), which is calculated by the ratio between the methacrylate groups and remaining methyl groups. By altering the initial molar ratio of the reagents, the ring-opening reaction of the epoxide functional group would occur to different extend, resulting in products of various DMs. Three different molar ratios were used to create low-methacrylated hyaluronic acid (LMHA-GM), medium-methacrylated hyaluronic acid (MMHA-GM) and high-methacrylated hyaluronic acid (HMHA-GM). The hydrogels were examined by ^{1}H NMR to evaluate their DMs, as shown in Supplement Fig. 1. The presence of the methacrylate group peaks at 5.6 and 6.0 ppm confirmed the methacrylation, as compared to hyaluronic acid in Supplement Fig. 1 d. The DMs were calculated by dividing the integration of peaks from the methacrylate group over that of the remaining methyl groups in hyaluronic acid at 1.7, 1.8 and 1.9 ppm [16]. The results are shown in Table 1. The LMHA-GM has a DM of 33.8%, which agrees with the values in previously reports [20].

3.2. Physical properties of HA-GM

The DMs of HA-GMs indicate the amount of functional groups for crosslinking among polymer chains. Physically, the degree of crosslinking will affect the water distribution within the hydrogel, which can be revealed from the pore sizes of the hydrogel after removing the water. To examine how the DMs affect the microscopic porous structures of the hydrogels, we compared SEM images of fully cured HA-GM hydrogels after drying. Theoretically, the hydrogels with higher DM will result in structures with smaller and less interconnected pores. As shown in Fig. 1(a), (b) and (c), with the lowest number of DM, the LMHA-GM forms the largest connected pores whereas MMHA-GM has much smaller and isolated pores. The HMHA-GM with the highest DM yielded the smallest pores. The pore sizes of each HA-GM were calculated as shown in Fig. 1(d).

The DMs of hydrogels will affect not only the pore sizes of the hydrogel, but also the physical properties of the gels, such as the swelling ratio. Less crosslinking sites will constitute to lower degree of crosslinking, hence less restrain on the hydrogel under osmotic pressure to swell after crosslinking. The ability of maintaining the structural integrity against swelling is crucial for bilayer construct since it will affect the cell-cell distance and signal transduction within the cell-hydrogel matrix. The less extend of swelling will essentially result in a closer packed matrix for cells to interact. With the least restrains, the LMHA-GM swells the most and eventually lose the shape after 5 days of incubation at 37 °C due to the lack of crosslinking sites to withstand the osmotic pressure. MMHA-GM has more crosslinking sites, hence it swells less than the LMHA-GM. With the highest degree of crosslinking, the HMHA-GM has the strongest ability to withhold the osmotic pressure, hence swells the least, as shown in Fig. 1(e). The porosities of hydrogels were calculated by the ratio between the volume of pores over the volume of the hydrogel. Due to the high swelling ratio of the HA-GMs, there is no significant difference in porosities of all hydrogels since majority of the hydrogel volume is filled by pores containing water.

Table 1
Degree of methacrylation of HA-GM synthesized by different glycidyl methacrylate to hyaluronic acid ratios.

Initial molar ratio	DM of final HA-GM
5:1	7.78%
10:1	25.54%
20:1	33.78%

Furthermore, the compressive modulus of the hydrogel is closely related to the DMs of hydrogels. The higher degree of crosslinking, the more tangling of polymer chains, resulting in stiffer gels under compression. Previous studies have demonstrated that the cell-hydrogel matrix should have the stiffness comparable to native retina, which is about 10–20 kPa, for the survival and development of *in vitro* retina [21,22]. The compressive modulus of each type of HA-GM hydrogel were measured and demonstrated in Fig. 1(f). With the highest DM, the HMHA-GM has the compressive modulus that is comparable to the native retina.

3.3. Hydrogel biocompatibility

To optimize the material composition for cell encapsulation, we investigated viability of RPEs in each HA-GM at different time periods (1 day, 3 days, 10 days). RGDs polypeptide motif was mixed with the hydrogels to improve the cell affinity. For LMHA-GM, the presence of cells did not alter the restrain against osmosis pressure within the matrix, hence it dissolved after 5 days of incubation. The cell viability in the remaining samples were analyzed using calcein AM and Ethidium Homodimer (L/D) assay following manufacturer's instruction. The results are shown in Fig. 2. RPEs in both remaining HA-GMs show high viability above 70%. Given its low swelling ratio and similar compressive modulus to native retina, the HMHA-GM was selected for the tissue construct.

3.4. Multilayer printing

To create a structure for maturation of PRs from fRPCs [23], we designed a construct to recapitulate the hierarchy of native retina, as shown in Fig. 3. Following the structure of native retinas, the base layer was designed with a thickness of 125 μm to resemble the epithelium tissue. The top layer was 250 μm tall to give room for the neurons to grow [24]. To validate the print, we created a sample where the bottom layer consists HMHA-GM hydrogel mixed with fluorescein isothiocyanate (FITC) dextran and a top layer mixed with tetramethylrhodamine isothiocyanate (TRITC) dextran. These dextran molecules would illustrate the printed structure due to their different fluoresce colors. The confocal image of the structure is shown in Fig. 3(c). This image demonstrated a bi-layer construct with distinct separation of the two layers.

3.5. Differentiation of fRPCs

In cell-hydrogel matrix, the microenvironment around the cells might affect their maturation. To investigate how the HA-GM will affect the maturation process, we used previously reported differentiation protocols on the fRPCs embedded in HA-GM [19]. The fRPCs were mixed with the HMHA-GM and printed in circular shapes. The fRPC-HMHA-GMs were placed in a cell culture incubator with dish and cultured with PR differentiation medium. During the two-week differentiation, small molecules and growth factors (IWP2, DAPT, purmorphamine, retinoid acid, taurin and bFGF) were able to penetrate the scaffold and induce cell reprogramming of fRPCs. As a result, the fRPCs have shown significant morphology change and turn into typical cone-, rod-like photoreceptor morphology, as shown in Supplement Fig. 2a. We used immunostaining of recoverine, a signature protein in the PRs, to verify maturation. The presence of recoverine in Supplement Fig. 2b confirmed the maturation of PRs, indicating successful differentiation of fRPC. This strategy has proven that the HA-GM would not alter the

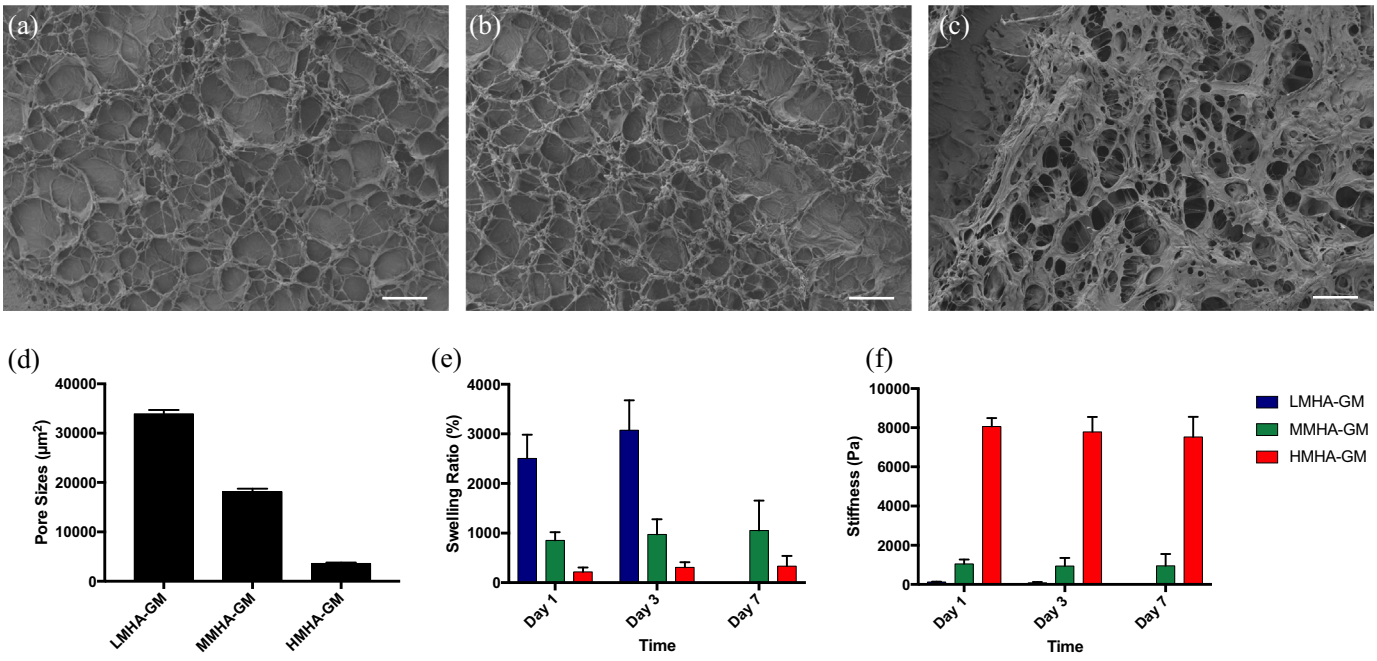

Fig. 1. Hydrogel characterization: SEM images of dried (a) LMHA-GM, (b) MMHA-GM, and (c) HMHA-GM. (d) The pore size of each HA-GM material indicated that with a higher DM, the resulting photocured HA-GM will have smaller pore sizes. (e) Compressive modulus and (f) swelling ratio of different HA-GMs after curing. Both results show that HMHA-GM has better matched physical properties to use as the ECM to build a multi-layered retina model *in vitro*. Scale bar of SEM images = 100 μm.

differentiation process of fRPCs. We then moved on to include the support from RPEs in the system by printing the bi-layer structure adjacent to the fRPCs.

3.6. Bi-layer construct for PR maturation

Results from previous tests indicated that HMHA-GM can be used for printing while supporting cell functions and differentiation. We then printed a bi-layer structure using the HMHA-GM with fRPCs and RPEs following guidance from native retina structure [24]. As shown in Supplement Fig. 3, the RPEs were encapsulated into HMHA-GM and printed at the bottom layer with the thickness of 125 μm. A second layer of HMHA-GM and fRPCs matrix were printed on top of the RPE layer. This design was also expected to introduce a gradient of nutrition and growth factor diffusion from the bottom RPE layer to the fRPC layer, which could guide the orientation of the cells to differentiate into

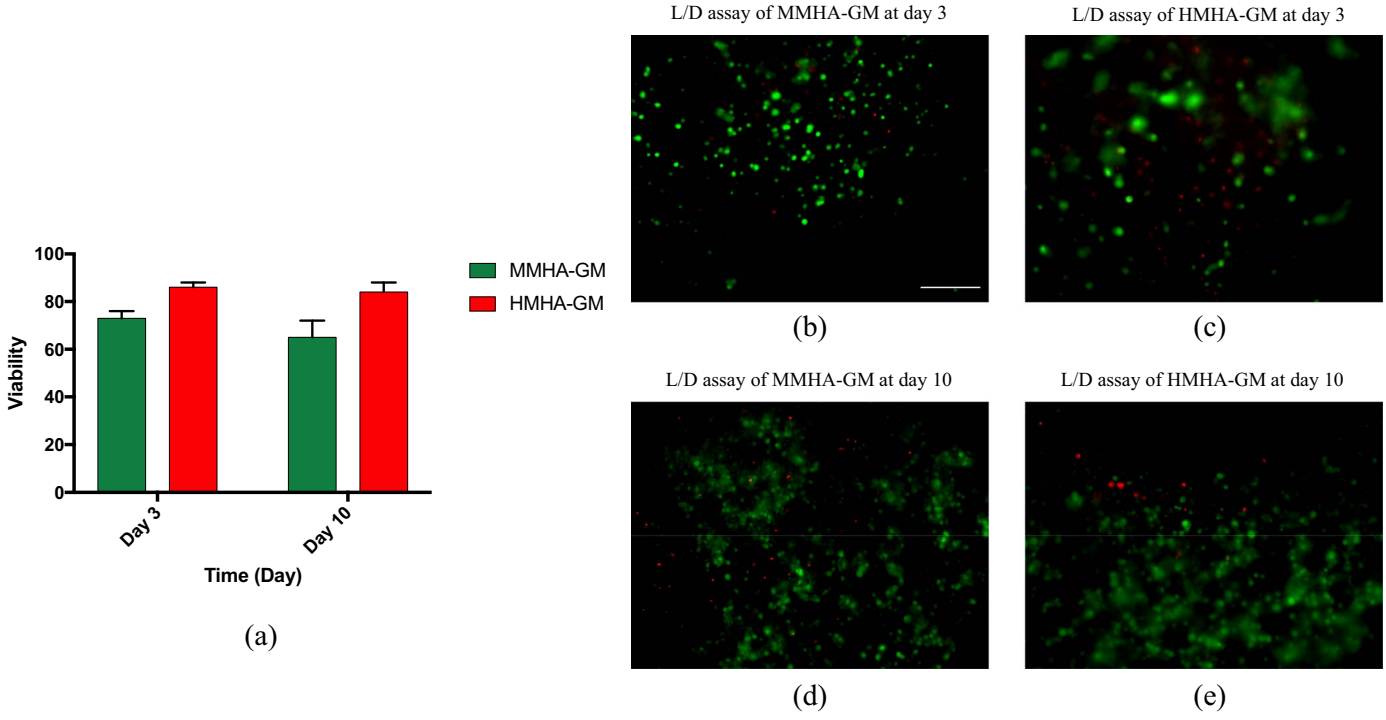

Fig. 2. Viability assay of RPEs encapsulated in MMHA-GM and HMHA-GM. The results shown that RPEs had the highest viabilities in HMHA-GM, which has stiffness close to native retina. Scale bar = 100 μm.

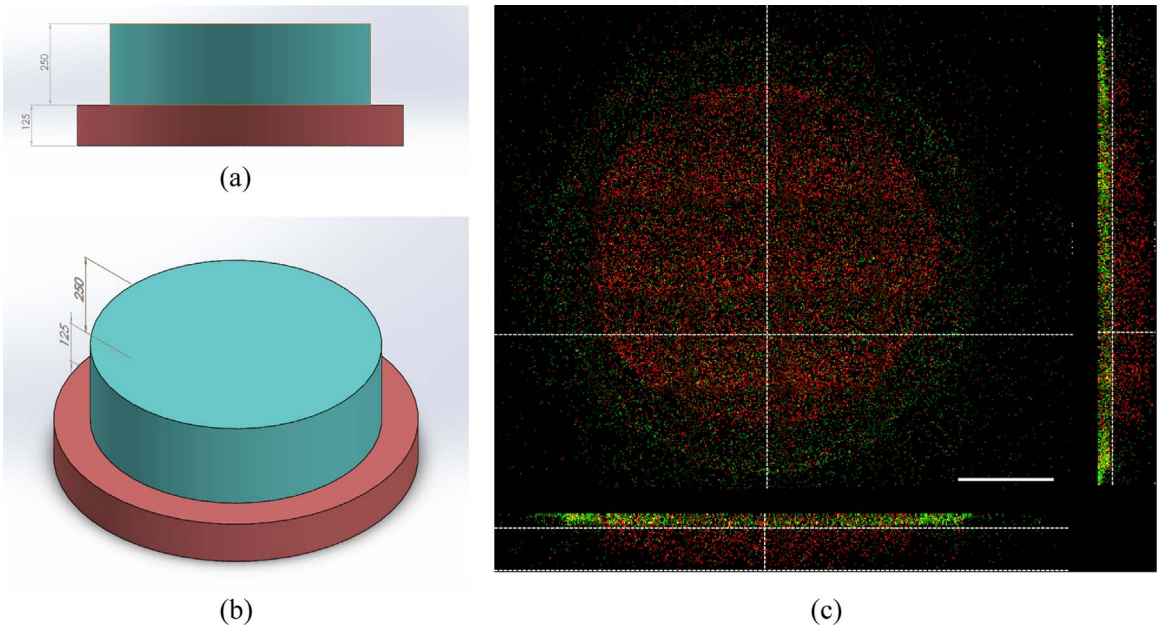

Fig. 3. Bilayer printing of fluorescent labelled hydrogels: (a) Top view and (b) side view of structural design from SolidWorks ® (c) Confocal fluorescent images showing bilayer construct. The printed structure recapitulated the structural design, indicating ability to construct multi-layered structure. Scale bar = 500 μm.

the highly ordered retinal cells including PRs, ganglion cells, and bipolar cells.

To maintain the stability of the cells during differentiation, we modified the differentiation media by adding SU5402 and IWP2 to inhibit FGF and Wnt pathway. These modifications have been proven to have a positive effect during differentiation [10]. With the adapted protocol, we observed PR maturation at day 14. As shown in Fig. 4(a), immunostaining of PR specific marker arrestin-3 indicated signature morphology of mature neurons [25]. The expansion of the outer segment demonstrated development of rod PRs. To further characterize the differentiation of fRPCs, we used western blot to examine the protein expression in the matrix. As shown in Fig. 4(b), the protein profile indicated abundance of both rhodopsin and M-opsin proteins after co-culturing for 14 days, which pinpointed the formation of both rod and cone PRs. Furthermore, we conducted real-time qPCR to verify the neuron formation. As shown in Fig. 4(c), the increase in presence of key neuron specific proteins such as Brn3, MATH5 and ISL-1 confirmed the maturation of PRs using the bi-layer construct.

4. Conclusions

In this work, we have demonstrated chemical synthesis of HA-GMs with different degrees of methacrylation. These HA-GMs exhibit distinctive physical properties such as pore sizes and compressive modulus. We further assessed viabilities of cells encapsulated in these hydrogels and found that the cells have better survival in hydrogels

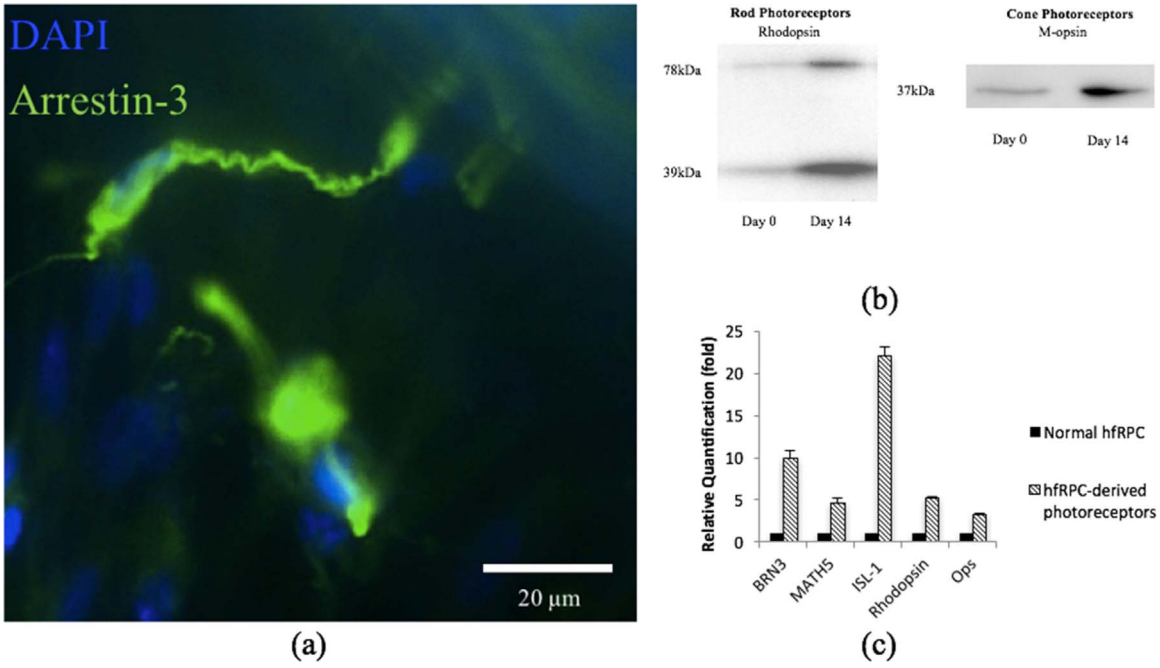

Fig. 4. Characterization of co-differentiation: (a) Immunostaining of cone PR specific protein arrestin-3 at day 14. (b) Western blot and (c) qPCR quantification of neuron-specific protein indicating PR maturation.

with mechanical properties close to native retina. Furthermore, we have demonstrated bioprinting of a bi-layer structure with cell-hydrogel matrix. After studying the expression of key proteins, we concluded that our co-culture system could recapitulate the native retinal development environment and enhance the maturation of PRs.

Acknowledgments

The work was supported in part by grants from the Department of Defense (W81XWH-14-1-0522), California Institute for Regenerative Medicine (RT3-07899), and National Institutes of Health (R01EB021857 and R21HD090662).

Appendix A. Supplementary material

Supplementary data associated with this article can be found in the online version at doi:10.1016/j.bprint.2018.e00029.

References

[1] N. Mitrousis, R.Y. Tam, A.E.G. Baker, D. Van Der Kooy, M.S. Shoichet, Hyaluronic acid-based hydrogels enable rod photoreceptor survival and maturation in vitro through activation of the mTOR pathway, Adv. Funct. Mater. 26 (2016) 1975–1985. http://dx.doi.org/10.1002/adfm.201504024.

[2] M. Eiraku, N. Takata, H. Ishibashi, M. Kawada, E. Sakakura, S. Okuda, K. Sekiguchi, T. Adachi, Y. Sasai, Self-organizing optic-cup morphogenesis in three-dimensional culture, Nature 472 (2011) 51–56. http://dx.doi.org/10.1038/nature09941.

[3] Y. Liu, R. Wang, T.I. Zarembinski, D. Ph, N. Doty, D. Ph, C. Jiang, C. Regatieri, X. Zhang, M.J. Young, D. Ph, The application of hyaluronic acid hydrogels to retinal progenitor, Cell Transplant. 19 (2013). http://dx.doi.org/10.1089/ten.tea.2012.0209.

[4] B.G.G. Ballios, M.J.J. Cooke, L. Donaldson, B.L.K.L.K. Coles, C.M.M. Morshead, D. van der Kooy, M.S.S. Shoichet, D. van der Kooy, M.S.S. Shoichet, A. Hyaluronan-Based, Injectable hydrogel improves the survival and integration of stem cell progeny following transplantation, Stem Cell Rep. 4 (2015) 1–15. http://dx.doi.org/10.1016/j.stemcr.2015.04.008.

[5] A.E. Sorkio, E.P. Vuorimaa-Laukkanen, H.M. Hakola, H. Liang, T.A. Ujula, J.J. Valle-Delgado, M. Österberg, M.L. Yliperttula, H. Skottman, Biomimetic collagen I and IV double layer Langmuir–Schaefer films as microenvironment for human pluripotent stem cell derived retinal pigment epithelial cells, Biomaterials 51 (2015) 257–269. http://dx.doi.org/10.1016/j.biomaterials.2015.02.005.

[6] P. Baranov, A. Michaelson, J. Kundu, R.L. Carrier, M. Young, Interphotoreceptor matrix-poly(-caprolactone) composite scaffolds for human photoreceptor differentiation, J. Tissue Eng. 5 (2014). http://dx.doi.org/10.1177/2041731414554139.

[7] C. Yvon, C.M. Ramsden, A. Lane, M.B. Powner, L. da Cruz, P.J. Coffey, A.-J.F. Carr, Using stem cells to model diseases of the outer retina, Comput. Struct. Biotechnol. J. (2015). http://dx.doi.org/10.1016/j.csbj.2015.05.001.

[8] C.M. Ramsden, M.B. Powner, A.-J.F. Carr, M.J.K. Smart, L. da Cruz, P.J. Coffey, Stem cells in retinal regeneration: past, present and future, Development 140 (2013) 2576–2585. http://dx.doi.org/10.1242/dev.092270.

[9] S.T.H. David, E. Buchholz, Embryonic stem cells/induced pluripotent stem cells derivation of functional retinal pigmented epithelium from induced, Stem Cells 27 (2009) 2427–2434. http://dx.doi.org/10.1002/July.

[10] J. Luo, P. Baranov, S. Patel, H. Ouyang, J. Quach, F. Wu, A. Qiu, H. Luo, C. Hicks, J. Zeng, J. Zhu, J. Lu, N. Sfeir, C. Wen, M. Zhang, V. Reade, S. Patel, J. Sinden, X. Sun, P. Shaw, M. Young, K. Zhanga, Human retinal progenitor cell transplantation preserves vision, J. Biol. Chem. 289 (2014) 6362–6371. http://dx.doi.org/10.1074/jbc.M113.513713.

[11] X. Ma, X. Qu, W. Zhu, Y.-S. Li, S. Yuan, H. Zhang, J. Liu, P. Wang, C.S.E. Lai, F. Zanella, G.-S. Feng, F. Sheikh, S. Chien, S. Chen, Deterministically patterned biomimetic human iPSC-derived hepatic model via rapid 3D bioprinting (201524510)Proc. Natl. Acad. Sci USA. (2016). http://dx.doi.org/10.1073/pnas.1524510113.

[12] B. Lorber, W.-K. Hsiao, I.M. Hutchings, K.R. Martin, Adult rat retinal ganglion cells and glia can be printed by piezoelectric inkjet printing, Biofabrication 6 (2014) 015001. http://dx.doi.org/10.1088/1758-5082/6/1/015001.

[13] W. Zhu, X. Ma, M. Gou, D. Mei, K. Zhang, S. Chen, 3D printing of functional biomaterials for tissue engineering, Curr. Opin. Biotechnol. 40 (2016) 103–112. http://dx.doi.org/10.1016/j.copbio.2016.03.014.

[14] X. Zhong, C. Gutierrez, T. Xue, C. Hampton, M.N. Vergara, L.-H. Cao, A. Peters, T.S. Park, E.T. Zambidis, J.S. Meyer, D.M. Gamm, K.-W. Yau, M.V. Canto-Soler, Generation of three-dimensional retinal tissue with functional photoreceptors from human iPSCs, Nat. Commun. 5 (2014) 4047. http://dx.doi.org/10.1038/ncomms5047.

[15] N.C. Hunt, D. Hallam, A. Karimi, C.B. Mellough, J. Chen, D.H. Steel, M. Lako, 3D culture of human pluripotent stem cells in alginate hydrogel improves retinal tissue development, Acta Biomater. (2016). http://dx.doi.org/10.1017/CBO9781107415324.004.

[16] J.A. Burdick, G.D. Prestwich, Hyaluronic acid hydrogels for biomedical applications, Adv. Mater. 23 (2011) 41–56. http://dx.doi.org/10.1002/adma.201003963.

[17] D.L. Hern, J.A. Hubbell, Incorporation of adhesion peptides into nonadhesive hydrogels useful for tissue resurfacing, J. Biomed. Mater. Res. 39 (1998) 266–276. http://dx.doi.org/10.1002/(SICI)1097-4636(199802)39:2<266::AID-JBM14>3.0.CO;2-B.

[18] K.C. Hribar, Y.S. Choi, M. Ondeck, A.J. Engler, S. Chen, Digital plasmonic patterning for localized tuning of hydrogel stiffness, Adv. Funct. Mater. 24 (2014) 4922–4926. http://dx.doi.org/10.1002/adfm.201400274.

[19] J.J. Zhao, H. Ouyang, J. Luo, S. Patel, Y. Xue, J. Quach, N. Sfeir, M. Zhang, X. Fu, S. Ding, S. Chen, K. Zhang, Induction of retinal progenitors and neurons from mammalian müller glia under defined conditions, J. Biol. Chem. 289 (2014) 11945–11951. http://dx.doi.org/10.1074/jbc.M113.532671.

[20] J. Baier Leach, K.A. Bivens, C.W. Patrick Jr., C.E. Schmidt, Photocrosslinked hyaluronic acid hydrogels: natural, biodegradable tissue engineering scaffolds, Biotechnol. Bioeng. 82 (2003) 578–589. http://dx.doi.org/10.1002/bit.10605.

[21] K.S. Worthington, L.A. Wiley, A.M. Bartlett, E.M. Stone, R.F. Mullins, A.K. Salem, C.A. Guymon, B.A. Tucker, Mechanical properties of murine and porcine ocular tissues in compression, Exp. Eye Res. 121 (2014) 194–199. http://dx.doi.org/10.1016/j.exer.2014.02.020.

[22] J. Hertz, R. Robinson, D. a. Valenzuela, E.B. Lavik, J.L. Goldberg, A tunable synthetic hydrogel system for culture of retinal ganglion cells and amacrine cells, Acta Biomater. 9 (2013) 7622–7629. http://dx.doi.org/10.1016/j.actbio.2013.04.048.

[23] T. Nakano, S. Ando, N. Takata, M. Kawada, K. Muguruma, K. Sekiguchi, K. Saito, S. Yonemura, M. Eiraku, Y. Sasai, Self-formation of optic cups and storable stratified neural retina from human ESCs, Cell. Stem Cell. 10 (2012) 771–785. http://dx.doi.org/10.1016/j.stem.2012.05.009.

[24] H. Kolb, Facts and Figures Concerning the Human Retina Size of Optic Nerve Head or Disc Cross Diameter of the Macula Cross Diameter of the Central Fovea from Foveal Rim to Foveal Rim Cross Diameter of Central Rod-free Area Central Region of Fovea Where There Are N, 2007, pp. 1–10.

[25] S. Schmitt, U. Aftab, C. Jiang, S. Redenti, H. Klassen, E. Miljan, J. Sinden, M. Young, Molecular characterization of human retinal progenitor cells, Investig. Ophthalmol. Vis. Sci. 50 (2009) 5901–5908. http://dx.doi.org/10.1167/iovs.08-3067.